nature physics

LETTERS

PUBLISHED ONLINE: 31 JULY 2011 | DOI: 10.1038/NPHYS2052

Arbitrarily shaped high-coherence electron bunches from cold atoms

A. J. McCulloch†, D. V. Sheludko†, S. D. Saliba, S. C. Bell, M. Junker, K. A. Nugent and R. E. Scholten*

Ultrafast electron diffractive imaging of nanoscale objects such as biological molecules[1,2] and defects in solid-state devices[3] provides crucial information on structure and dynamic processes: for example, determination of the form and function of membrane proteins, vital for many key goals in modern biological science, including rational drug design[4]. High brightness and high coherence are required to achieve the necessary spatial and temporal resolution, but have been limited by the thermal nature of conventional electron sources and by divergence due to repulsive interactions between the electrons, known as the Coulomb explosion. It has been shown that, if the electrons are shaped into ellipsoidal bunches with uniform density[5], the Coulomb explosion can be reversed using conventional optics, to deliver the maximum possible brightness at the target[6,7]. Here we demonstrate arbitrary and real-time control of the shape of cold electron bunches extracted from laser-cooled atoms. The ability to dynamically shape the electron source itself and to observe this shape in the propagated electron bunch provides a remarkable experimental demonstration of the intrinsically high spatial coherence of a cold-atom electron source, and the potential for alleviation of electron-source brightness limitations due to Coulomb explosion[6].

Carbon nanotube field emitters are at present the brightest available electron sources but must operate at low currents to avoid Coulomb expansion and are therefore not suitable for ultrafast imaging. Limited bunch shaping has been demonstrated with photoemission sources[7,8], which use high-energy laser pulses to generate electrons at high current. Combined with longitudinal bunch compression, sub-100 fs pulses have been obtained with sufficient brightness for diffraction studies of gold[8,9]. However, large increases in brightness are needed for single-shot imaging of weakly scattering materials such as biological molecules, and further increases in the brightness of intrinsically hot photoemission sources will be difficult.

Recent simulations[10,11] and experiments[12] show that photoionization of a cold atom cloud can produce cold electron bunches with high coherence and current. Electrons are extracted by near-threshold photoionization of atoms that have been laser-cooled to microKelvin temperature[13]. We demonstrate here that the extracted electron bunches have extremely small transverse momentum, and show that the source has quasi-homogeneous rather than thermal coherence properties; that is, unlike conventional photocathode sources, the transverse locations of the cold electrons remain strongly correlated to their original location at the source.

In addition, the internal structure of the atoms that form the underlying electron source provides a unique tool for three-dimensional control of the electron bunch shape[5]. We show that it is possible to engineer the spatial profiles of the incident excitation and photoionization laser beams to control the shape of the ionized gas cloud and hence that of the extracted electron bunches in three dimensions. We demonstrate real-time arbitrary shaping to create complex electron density distributions, and show that, because of the extremely small transverse momentum of the electrons, the bunch shape is preserved after propagation, without focussing optics. The preservation of the spatial structure of the cold electron beam shows that high-resolution measurement of electron diffraction will be possible without requiring beam expansion and associated loss of flux to increase the transverse coherence. Conventional photocathode sources offer high brightness and the ability to pattern the electron emission in two dimensions, but low transverse coherence due to their inherently high electron temperature, such that any pattern immediately diffuses. Although the pattern could subsequently be recovered with imaging optics, the transverse spatial coherence would always remain low, limiting the applicability for diffractive imaging. We also use the arbitrary shaping capability of the cold-atom electron source to measure the high transverse spatial coherence length of the electrons.

In our experiments, laser-cooled rubidium atoms ($T = 70\,\mu\mathrm{K}$) were photoionized by illumination with a resonant 780 nm excitation laser, followed by a 5 ns 480 nm ionization laser pulse (Fig. 1). The electrons were accelerated in a uniform electric field ($F = 40\,\mathrm{kV\,m^{-1}}$, distance 2.5 cm, final energy 1 keV), and the spatial distribution of the electron pulse was observed after the pulse had propagated 21.5 cm in a null field. A spatial phase modulator was used to control the intensity profile of the excitation laser beam at the cold-atom target, forming a shaped charge cloud on ionization (see Methods). An example of a complex electron pattern is shown in Fig. 1. The density distribution of the electrons extracted from the shaped cloud directly reflects the excitation-laser intensity profile, even after propagation by 24 cm (14 ns time of flight). The cold electron bunches have extremely small transverse momentum, demonstrating high coherence, and quasi-homogeneous rather than thermal source properties (see Methods). For a quasi-homogeneous source[14], the transverse coherence length L_c can be related to the transverse momentum spread, and hence the temperature T, through[10]

$$L_c = \hbar/\sqrt{m_e k_B T} \tag{1}$$

Note that the transverse coherence length is determined by the temperature of the electrons and is independent of the acceleration energy. Equation (1) predicts that the transverse coherence length decreases with increasing temperature, and therefore with decreasing photoionization wavelength. At the very low temperatures possible with a cold atom source, the electrons have negligible transverse momentum, and so the electron distribution at our detector will closely match the excitation profile. As the electron temperature is increased, by increasing the energy of the ionizing photons, the distribution at the detector will blur owing to the thermal diffusion during propagation.

ARC Centre of Excellence in Coherent X-ray Science, School of Physics, The University of Melbourne, Victoria 3010, Australia. †These authors contributed equally to this work. *e-mail: scholten@unimelb.edu.au.

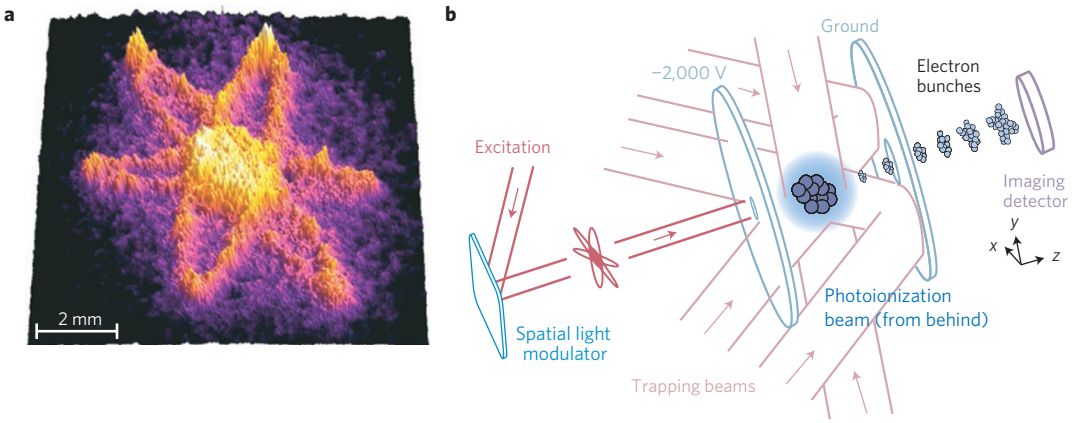

Figure 1 | Arbitrary electron density distribution bunches using spatially structured photoionization of a cold atom cloud. a, False-colour surface rendering of relative electron density for a shaped electron bunch after propagation by 24 cm, measured with a microchannel plate, phosphor screen and CCD (charge-coupled device) camera. **b**, Atoms are laser cooled and trapped and then photoionized with a combination of a 780 nm laser beam shaped by a spatial light modulator and a uniform-intensity-profile 480 nm laser pulse. Electrons produced in the region of overlap between atoms, excitation and photoionization beams are propelled to a microchannel plate and phosphor screen detector, imaged with a cooled interline transfer CCD camera.

The electron temperature and coherence can be quantified from the change in bunch structure after propagation. Figure 2a shows the spatial-resolution degradation as the photoionization-laser wavelength was decreased by 2.6 nm, increasing the electron energy and temperature by 15 meV and 170 K, until the structure is no longer discernible. The preservation of the detailed complex pattern at low temperature underscores the remarkable coherence that can be obtained with a cold-atom electron source.

To more precisely quantify the effects of temperature on spatial coherence, the excitation-laser profile was adjusted to produce uniform-density electron bunches with sharply defined edges. The blurring of the edges as a function of excess excitation energy provides a more precise test for the loss of structure with electron temperature (Fig. 2b). The edge width before propagation is defined by the resolution of the excitation intensity profile, which in turn is defined by the optical resolution of the excitation-laser imaging system, approximately 10 μm.

With the ionization-laser wavelength at the field-free ionization wavelength, λ_0, we expect to see cold electrons from directly ionized atoms, but also electrons from atoms that are excited to Rydberg states and then ionized owing to the ambient external electric field between the accelerator electrodes. In a non-zero ambient electric field, excitation at the field-free ionization wavelength produces hot electrons, which gain excess energy contributed from the ambient electric field. The coldest electrons are therefore formed by excitation to a Rydberg state (see Methods). For our field strength the calculated ionization threshold wavelength is 481.885 nm (see Methods). The observed threshold of 481.775 nm is lower, consistent with observations for other atomic species[15].

The edge-resolution measurements can be used to determine an upper limit to electron temperature and a lower limit to source coherence. Equating the transverse thermal velocity of the electron cloud to the angular spread after propagation yields an expression for the spatial derivative at the boundary[16]:

$$\frac{\mathrm{d}Q_\mathrm{e}}{\mathrm{d}r} = e\kappa \frac{d_1}{2d_1 + d_2} \sqrt{\frac{eF}{d_1 [k_\mathrm{B} T_0 + \Delta E]}} \qquad (2)$$

where Q_e is the detector signal proportional to charge, r is the radial coordinate, d_1 is the distance through which the cloud is accelerated by an electric field of strength F and d_2 is the free propagation distance from accelerator to detector. ΔE is the excess energy of the electrons (see Methods), determined from the experimentally observed ionization shift, such that the sharpest electron bunch corresponds to $\Delta E = 0$. Both κ and T_0 are fitting parameters; κ is the linear magnification, and T_0 is the minimum electron temperature, fundamentally limited by intrinsic heating processes during ionization. Figure 2c plots the intensity derivative across the boundary as a function of excess ionization energy for the quasi-uniform electron bunches. The extracted upper limit to the minimum electron temperature of $T_0 < (10 \pm 5)$ K is consistent with other measurements for electrons extracted by photoionization of cold atoms[17].

Using equation (1), the intrinsic transverse coherence length of the electron source with temperature $T < (10 \pm 5)$ K is then $L_\mathrm{c} > (10 \pm 3)$ nm. Our direct measurement shows that the transverse coherence length of cold-atom electron sources is sufficient for diffractive imaging of nanocrystals of many proteins and solid-state structures of interest, and even small viruses[10]. The spatial coherence length can be increased with reduced temperature or by expansion of the bunch.

Flexible control of the bunch shape through the scheme described here was essential for creation of the uniform-density sharply defined electron bunches used to measure the source coherence. The false-colour surface rendering of the relative electron density of Fig. 1a shows two dominant contributions to the bunch shape: the intensity profile of the shaped excitation laser beam, and also the initial atomic density distribution of the cold atom cloud. The latter is manifest as a Gaussian, rather than uniform, envelope modulating the binary intensity profile of the excitation laser beam. To generate uniform bunches, the cold atom cloud was imaged before ionization and the measured atom distribution used to calculate a revised excitation-laser profile, to reduce the excitation fraction where the atom distribution is high, and increase excitation in regions of low atomic density (see Methods).

With such flexible control of bunch shaping, real-time feed-forward correction for the non-uniformity of the cold-atom distribution is possible. The illumination can be changed from one excitation pulse to the next, and will therefore also enable feedback correction of electron bunch shape from shot to shot. A movie (see Supplementary Information) shows a dynamic animation similar to Fig. 1a, where schematic 'electrons' are seen to orbit the 'atom', and a 'photon' ionizes the atom. Every pulse of the ionization laser illuminates a different distribution of excited-state atoms, at a rate of 10 Hz.

The transverse brightness at the source is given by[18]

$$B_\perp = \frac{I_\mathrm{p} m_\mathrm{e} c^2}{4\pi^2 \sigma_x \sigma_y k_\mathrm{B} T}$$

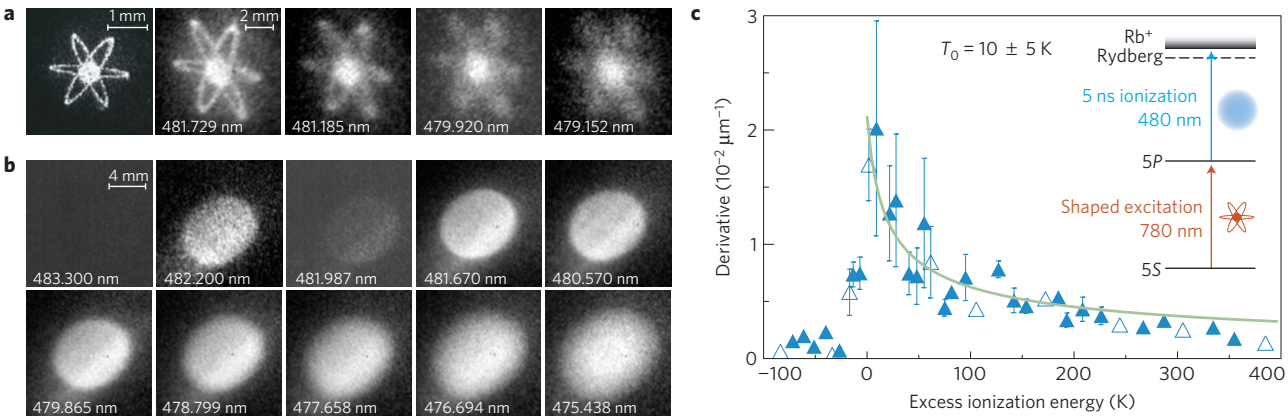

Figure 2 | Effect of electron temperature on structural degradation. a, Excitation-laser intensity profile (left), and sequence of detected electron bunches extracted with varying excess ionization energies. A rise of only 25 K in electron temperature leads to significant distortion of the complex image. Images are 9 mm × 9 mm averaged over 30 shots. **b**, Sequence of quasi-uniform electron bunches for varying ionization-laser wavelength, used to measure the source temperature. The excitation to Rydberg levels is apparent at $\lambda = 482.20$ nm, well above the free-field ionization wavelength, $\lambda_0 = 479.059$ nm. Images are 13.5 mm × 13.5 mm averaged over 20 shots. **c**, Electron bunch edge width. The open triangles correspond to the images in **b**. The error bars indicate one standard deviation, including statistical and systematic uncertainties. An upper limit to source temperature is extracted by fitting equation (2) (solid line) to the data with excess ionization energy $\Delta E_c \geq 0$ K. Inset: The relevant energy levels and transitions in rubidium.

where σ is the root mean squared source size and I_p is the peak electron current. For $N_e = 10^5$ electrons at energy 1 keV in a 5 ns pulse and a source size of 1 mm, $T < 10$ K gives a lower limit to the transverse brightness of $B_\perp > 10^7$ A m^{-2} sr^{-1}. The brightness of the pulse can be increased by reducing the bunch length, and a short bunch length is also necessary for ultrafast electron diffraction applications. The length was limited in our set-up by the 5 ns photoionization-laser pulse duration, but in principle this can be reduced to picoseconds before the transform-limited bandwidth of the laser significantly affects the electron temperature. Standard radiofrequency accelerator compression techniques can then reduce the bunch length to below 100 fs (refs 11,19). The energy spread of the electron bunches can be estimated from the length of the initial electron bunch along the electric field between the two accelerator electrodes. For the results presented here, the length is 1 mm and the field is 40 kV m^{-1}, and thus there is a difference in acceleration of 40 V between electrons at the front and rear of the bunch, 4% of the final electron energy. The spread can be largely eliminated by using a time-dependent field[20].

The beam-shaping techniques and electron coherence described here realize an important advance in the production of high-brightness uniform ellipsoidal electron bunches. We have shown that electrons with sufficiently high coherence at the source are analogous to a quasi-homogeneous optical wavefield defined by two variables, rather than four as required to describe a general partially coherent source. The electron propagation is therefore more tractable to analytic treatment, for example for calculating diffraction and retrieving structure from diffraction patterns. Conceptually, the effective source size at some point in the propagated electron beam is defined by the momentum spread at the source, and not by the physical size of the source or of the electron beam, enabling coherent diffractive imaging with an extended source.

Using control of the photoionization-laser beam profile, we have also defined the bunch shape along the propagation direction (see Supplementary Information), for example to create sharp-edged 'pancake' cylindrical electron bunches, which, even when accounting for stochastic interactions[11], can expand naturally to form ideal uniform ellipsoidal electron bunches[6]. Optical bunch-shaping provides a very powerful tool for characterization and optimization of the source in real time, for example to measure the coherence and for feed-forward correction as reported here, and in future, active feedback control. The otherwise intractable problems imposed by transverse and longitudinal Coulomb expansion can then be reversed, to increase the brightness of electron injectors for synchrotrons, X-ray free-electron lasers and particle accelerators, and for high-resolution dynamic electron diffractive imaging. The same principles could also be applied to cold-atom ion sources for imaging or focused ion beam milling[21,22], where the Coulomb explosion is less important, but controlling the illumination[23] may enable optimization of resolution and throughput of the ion optics.

Methods

Experimental apparatus and techniques. Approximately 10^9 cold rubidium-85 atoms were collected in a magneto-optical trap, loaded from a Zeeman slower[24] attached to an effusive source. The magneto-optical trap was formed between two electrodes to enable electrostatic extraction of the cold atoms (Fig. 1). A quasi-mirror magneto-optical trap design was implemented, with one electrode used as a mirror to reflect four of the atom cooling and trapping laser beams, and the other electrode formed from a transparent conductive window[21]. Photoionization was carried out as a two-step process, with a resonant excitation laser (780 nm) to excite atoms from the $5S_{1/2}$ ($F = 3$) ground state to the $5P_{3/2}$ ($F = 4$) excited state (Fig. 2c). A tunable photoionization laser (480 nm) coupled the excited-state atoms to the ionization continuum, or to Rydberg states that were subsequently field-ionized, in either case leading to the formation of ultracold ions and electrons. The excess energy of the electrons is given by[25]

$$\Delta E = hc\left[\frac{1}{\lambda} - \left(\frac{1}{\lambda_0} - 4\,\mathrm{Ry}\sqrt{\frac{F}{F_0}}\right)\right]$$

where λ is the ionization-laser wavelength, $\lambda_0 = 479.059$ nm (ref. 26) is the wavelength equivalent to the field-free ionization energy, $4hc\,\mathrm{Ry}\sqrt{F/F_0}$ is the shift in ionization threshold due to d.c. field ionization of Rydberg states, Ry is the Rydberg constant, F is the magnitude of the electric field and F_0 is the atomic unit for electric field[27].

For manipulation of the density distribution of the charge cloud, a spatial light modulator (SLM, Holoeye Pluto NIR2 1920 × 1080 8 μm pixels, eight-bit phase only) was used to control the intensity profile of the excitation laser beam. To generate the required diffracted laser intensity, the SLM was programmed to show a holographic phase mask. Phase patterns were computed using an iterative Gerchberg–Saxton algorithm optimized for calculation of holographic phase masks[28].

The photoionization laser beam was expanded such that the intensity was uniform to within 3% over the entire cold-atom sample. The combination of excitation and photoionization beams forms a cold ionized gas cloud, with the density distribution of the cloud determined by the density of the atoms before ionization, and the intensity cross-section of the excitation laser beam. The shaped charged-particle distribution was created along the axis of acceleration, so that the extracted electron bunch density was proportional to the excitation-laser intensity profile. The electrons were extracted with a constant electrostatic field, detected with a microchannel-plate electron multiplier and phosphor screen, and imaged

with a cooled interline transfer CCD camera. Typically 10^5 electrons (20 fC) were extracted per photoionization pulse. Fully three-dimensional bunch shaping was demonstrated by controlling the profile of the ionization laser beam, incident orthogonal to the electron propagation axis (see Supplementary Information).

Feed-forward bunch-shape correction. Given the integrated column density of the ground-state atom cloud before ionization, $\rho(x,y)$, the required intensity profile $I(x,y)$ for an arbitrary excited-state distribution $\rho_e(x,y)$ can be calculated through the optical Bloch equations[15]:

$$I(x,y)=\frac{1}{\Gamma^2}\left[\frac{I_s\left(\Gamma^2+4\Delta^2\right)}{1-2\rho_e(x,y)}-I_s\Gamma^2-4\Delta^2 I_s\right]$$

where Γ is the natural line-width, Δ is the detuning from atomic resonance and I_s is the saturation intensity. For feed-forward shaping, the atom cloud column density $\rho(x,y)$ was measured using near-resonant diffraction contrast imaging[29].

For quantitative examination of the effects of electron temperature, gradients across the edge of the clouds were calculated using a least-squares linear fit to the relevant section of a line profile from the image. Each data point represents an average of 1,000 gradients across the bunch edge. Each image was normalized to a central electron signal of unity, and corrected for elliptical distortion, before the gradients were calculated, to eliminate intensity variation and image distortion effects. The error bars in Fig. 2c show the standard deviation of the 1,000 gradients at each point. The uncertainty in temperature combines the systematic error derived from the combination of detector resolution (25 μm) and electron optics geometry, and the calculated least-squares fitting error of the data to equation (2). The extracted temperature is strongly dependent on measurements near threshold, such that discrepancy at high excess energy has little impact on T_0.

Quasi-homogeneous source coherence. The electron bunch is a two-dimensional cloud of electrons with temperature T and Maxwellian momentum distribution:

$$D(\mathbf{p}_\perp,p_{0\|})=\left(\frac{1}{2\pi m_e k_B T}\right)^{3/2}\exp\left[-\frac{|\mathbf{p}_\perp|^2+p_{0\|}^2}{2m_e k_B T}\right]$$

where $(\mathbf{p}_\perp,p_{0\|})$ are the electron momentum components transverse and parallel to the propagation axis respectively. Momentum component p_F is added owing to an electric field along the bunch propagation axis; the longitudinal momentum becomes $p_\| = p_{0\|}+p_F$, and the phase-space density of the accelerated bunch is then

$$W(\mathbf{r}_\perp,\mathbf{p})=\left(\frac{1}{2\pi m_e k_B T}\right)^{\frac{3}{2}}\exp\left[-\frac{|\mathbf{p}_\perp|^2+\left(p_\|-p_F\right)^2}{2m_e k_B T}\right]J_e(\mathbf{r}_\perp)$$

where $J_e(\mathbf{r}_\perp)$ is the current density. As $p_F \gg p_{||}$, the distribution has a well-defined momentum component along the propagation direction, analogous to a quasi-monochromatic paraxial optical wave field. For such a field, the mutual optical intensity is related to the phase-space distribution by[14]

$$J\left(\mathbf{r}_\perp+\frac{\mathbf{x}}{2},\mathbf{r}_\perp-\frac{\mathbf{x}}{2}\right)=\int W(\mathbf{r}_\perp,\mathbf{p}_\perp)\exp\left[i\frac{\mathbf{x}\cdot\mathbf{p}_\perp}{\hbar}\right]\mathrm{d}\mathbf{p}_\perp$$

and thus

$$J(\mathbf{r}_\perp)=\frac{J_e(\mathbf{r}_\perp)}{\sqrt{2\pi m_e k_B T}}\exp\left[-\frac{m_e k_B T}{2\hbar^2}|\mathbf{x}|^2\right]=\frac{J_e(\mathbf{r}_\perp)}{\sqrt{2\pi m_e k_B T}}\exp\left[-\frac{|\mathbf{x}|^2}{2L_c^2}\right]$$

where $\mathbf{r}_\perp=(\mathbf{r}_1+\mathbf{r}_2)/2$ and $\mathbf{x}=(\mathbf{r}_1-\mathbf{r}_2)$. This is the mutual optical intensity of a quasi-homogeneous source with transverse coherence length L_c given by equation (1) (refs 14,30). A quasi-homogeneous wave field is defined by two variables rather than four, and therefore more tractable to analytic treatment, for example for calculating diffraction and retrieving structure from diffraction patterns. Conceptually, the effective source size at some point in the electron beam is defined by the momentum spread (temperature) at the source, and not by the physical size of the source or of the electron beam.

Received 13 December 2010; accepted 22 June 2011; published online 31 July 2011

References

1. Dwyer, J. R. *et al.* Femtosecond electron diffraction: 'Making the molecular movie'. *Phil. Tran. R. Soc. A* **364,** 741–778 (2006).
2. Williamson, J. C., Cao, J., Ihee, H., Frey, H. & Zewail, A. H. Clocking transient chemical changes by ultrafast electron diffraction. *Nature* **386,** 159–162 (1997).
3. Siwick, B. J., Dwyer, J. R., Jordan, R. E. & Miller, R. J. D. An atomic-level view of melting using femtosecond electron diffraction. *Science* **302,** 1382–1385 (2003).
4. Pinto, L. H., Holsinger, L. J. & Lamb, R. A. Influenza virus M2 protein has ion channel activity. *Cell* **69,** 517–528 (1992).
5. van der Geer, S. B. *et al.* Simulated performance of an ultracold ion source. *J. Appl. Phys.* **102,** 094312 (2007).
6. Luiten, O. J., van der Geer, S. B., de Loos, M. J., Kiewiet, F. B. & van der Wiel, M. J. How to realize uniform three-dimensional ellipsoidal electron bunches. *Phys. Rev. Lett.* **93,** 094802 (2004).
7. Musumeci, P., Moody, J. T., England, R. J., Rosenzweig, J. B. & Tran, T. Experimental generation and characterization of uniformly filled ellipsoidal electron-beam distributions. *Phys. Rev. Lett.* **100,** 244801 (2008).
8. van Oudheusden, T. *et al.* Compression of subrelativistic space-charge-dominated electron bunches for single-shot femtosecond electron diffraction. *Phys. Rev. Lett.* **105,** 264801 (2010).
9. Tokita, S. *et al.* Single-shot femtosecond electron diffraction with laser-accelerated electrons: Experimental demonstration of electron pulse compression. *Phys. Rev. Lett.* **105,** 215004 (2010).
10. van Oudheusden, T. *et al.* Electron source concept for single-shot sub-100 fs electron diffraction in the 100 keV range. *J. Appl. Phys.* **102,** 093501 (2007).
11. van der Geer, S. B., de Loos, M. J., Vredenbregt, E. J. D. & Luiten, O. J. Ultracold electron source for single-shot, ultrafast electron diffraction. *Micro. Microanal.* **15,** 282–289 (2009).
12. Claessens, B. J., Reijnders, M. P., Taban, G., Luiten, O. J. & Vredenbregt, E. J. D. Cold electron and ion beams generated from trapped atoms. *Phys. Plasmas* **14,** 093101 (2007).
13. Killian, T. C. *et al.* Creation of an ultracold neutral plasma. *Phys. Rev. Lett.* **83,** 4776–4779 (1999).
14. Nugent, K. A. Coherent methods in the X-ray sciences. *Adv. Phys.* **59,** 1–99 (2010).
15. Allen, L. & Eberly, J. H. *Optical Resonance and Two-Level Atoms* (Dover Publications, 1987).
16. Sheludko, D. V. Shaped electron bunches from ultracold plasma, Ph.D. thesis, Univ. Melbourne (2010). http://repository.unimelb.edu.au/10187/9228.
17. Taban, G. *et al.* Ultracold electron source for single-shot diffraction studies. *Europhys. Lett.* **91,** 46004 (2010).
18. Reiser, M. *Theory and Design of Charged Particle Beams* (Wiley-VCH, 2008).
19. van Oudheusden, T. *et al.* Compression of subrelativistic space-charge-dominated electron bunches for single-shot femtosecond electron diffraction. *Phys. Rev. Lett.* **105,** 264801 (2010).
20. Reijnders, M. P. *et al.* Phase-space manipulation of ultracold ion bunches with time-dependent fields. *Phys. Rev. Lett.* **105,** 034802 (2010).
21. Hanssen, J. L., Dakin, E. A., McClelland, J. J. & Jacka, M. Using laser-cooled atoms as a focused ion beam source. *J. Vac. Sci. Technol. B* **24,** 2907–2910 (2006).
22. Steele, A., Knuffman, B., McClelland, J. & Orloff, J. Focused chromium ion beam. *J. Vacuum Sci. Technol. B* **28,** C6F1 (2010).
23. Ito, R. & Okazaki, S. Pushing the limits of lithography. *Nature* **406,** 1027–1031 (2000).
24. Bell, S. C. *et al.* A slow atom source using a collimated effusive oven and a single-layer variable pitch coil Zeeman slower. *Rev. Sci. Inst.* **81,** 013105 (2010).
25. Merkt, F. *et al.* High Rydberg states of argon: Stark effect and field-ionization properties. *J. Phys. B* **31,** 1705–1724 (1998).
26. Steck, D. A. Rubidium 85 D-line data. Los Alamos National Laboratory, available online at http://steck.us/alkalidata (2008).
27. Baranov, L. Y., Kris, R., Levine, R. D. & Even, U. On the field ionization spectrum of high Rydberg states. *J. Chem. Phys.* **100,** 186–196 (1994).
28. Johansson, M. & Bengtsson, J. Robust design method for highly efficient beam-shaping diffractive optical elements using an iterative-Fourier-transform algorithm with soft operations. *J. Mod. Opt.* **47,** 1385–1398 (2000).
29. Sheludko, D. V. *et al.* State-selective imaging of cold atoms. *Phys. Rev. A* **77,** 033401 (2008).
30. Nugent, K. A. Quasi-homogeneous fields: A van Cittert–Zernike theorem and the recovery of correlations from intensity. *Opt. Commun.* **118,** 9–13 (1995).

Acknowledgements

We thank E. J. D. Vredenbregt and O. J. Luiten for discussions and advice. This work was supported by the Australian Research Council Federation Fellowship scheme and Australian Research Council Discovery Project DP1096025.

Author contributions

A.J.M. and D.V.S. contributed equally to this work; they executed the experiments and acquired and analysed the data; S.D.S. contributed to the analysis of electron coherence; D.V.S., M.J. and S.C.B. designed and constructed the apparatus; K.A.N. contributed to the theoretical analysis; A.J.M., D.V.S., K.A.N. and R.E.S. wrote the manuscript; R.E.S. conceived and directed the project.

Additional information

The authors declare no competing financial interests. Supplementary information accompanies this paper on www.nature.com/naturephysics. Reprints and permissions information is available online at http://www.nature.com/reprints. Correspondence and requests for materials should be addressed to R.E.S.